6-1-2014

Phase Control and Fast Start-Up of a Magnetron Using Modulation of an Addressable Faceted Cathode

J. Browning
Boise State University

S. Fernandez-Gutierrez
Boise State University

M. C. Lin
Tech-X Corporation

D. N. Smithe
Tech-X Corporation

J. Watrous
TechFlow

Phase control and fast start-up of a magnetron using modulation of an addressable faceted cathode

J. Browning,[1,a)] S. Fernandez-Gutierrez,[1] M. C. Lin,[2] D. N. Smithe,[2] and J. Watrous[3]
[1]*Electrical and Computer Engineering Department, Boise State University, Boise, Idaho 83725, USA*
[2]*Tech-X Corporation, Boulder, Colorado 80303, USA*
[3]*TechFlow, Albuquerque, New Mexico 87106, USA*

(Received 15 April 2014; accepted 1 June 2014; published online 12 June 2014)

The use of an addressable, faceted cathode has been proposed as a method of modulating current injection in a magnetron to improve performance and control phase. To implement the controllable electron emission, five-sided and ten-sided faceted planar cathodes employing gated field emitters are considered as these emitters could be fabricated on flat substrates. For demonstration, the conformal finite-difference time-domain particle-in-cell simulation, as implemented in VORPAL, has been used to model a ten-cavity, rising sun magnetron using the modulated current sources and benchmarked against a typical continuous current source. For the modulated, ten-sided faceted cathode case, the electrons are injected from three emitter elements on each of the ten facets. Each emitter is turned ON and OFF in sequence at the oscillating frequency with five emitters ON at one time to drive the five electron spokes of the π-mode. The emitter duty cycle is then 1/6th the Radio-Frequency (RF) period. Simulations show a fast start-up time as low as 35 ns for the modulated case compared to 100 ns for the continuous current cases. Analysis of the RF phase using the electron spoke locations and the RF magnetic field components shows that the phase is controlled for the modulated case while it is random, as typical, for the continuous current case. Active phase control during oscillation was demonstrated by shifting the phase of the electron injection 180° after oscillations started. The 180° phase shift time was approximately 25 RF cycles.
 [http://dx.doi.org/10.1063/1.4883395]

High power microwave oscillators and amplifiers are used in many applications including radar, communications, defeat of improvised explosives, and electronic warfare.[1] Crossed-field devices including magnetrons[2] and crossed-field amplifiers[1] have been used for many decades in a number of these applications. Improvements in power density, device efficiency, phase-locking or control, and reduced, consistent startup times are of particular interest. Conventional magnetrons provide RF power in the tens to hundreds of kW range.[1] These coaxial structures consist of an electron-supplying cathode at the center and a surrounding anode, forming a slow-wave structure. These devices have static radial electric fields, **E**, and axial magnetic fields, **B**, perpendicular to each other, and electrons drift in the device at the $\mathbf{E} \times \mathbf{B}$ drift velocity. Electrons cycloid azimuthally around the cylindrical structure. The electron motion results in a rotating hub around the cathode. The collective behavior of these electrons causes a perturbation which then interacts with the slow wave circuit. This process feedbacks and induces bunching of the electrons until spokes form and the device is oscillating. The operating frequency is determined by the resonant modes of the slow wave circuit and the synchronous velocity of the electrons.

Magnetrons use either thermionic[1] or field emission cathodes.[3] Thermionic cathodes are very reliable and proven but offer no method of temporal control over electron injection. Field emission cathodes rely on the anode to cathode electric field for emission, so no temporal or addressable control is possible. Research into transparent or multiple cathodes[4–6] has demonstrated a degree of spatial control of current injection and reduced startup times. In a previous work,[7] we proposed the use of gated, vacuum field emitter arrays in place of thermionic cathodes. Other groups[8] have also demonstrated the use of gated field emitters in traveling wave tubes. In our approach, the emitters would be placed below the interaction space in a shielded structure. Because the gated emitters would need to be fabricated on flat plates, the proposed cathode would be made up of five or ten facet plates containing the field emission cathode. These ideas were explored in the prior work[7] including simulation of the faceted cathode structure in a ten-cavity, rising sun magnetron. Those simulations were performed using the 3D particle-in-cell (PIC) code ICEPIC.[9] In this current work, we look at the effects of temporally modulating the electron injection using discrete (addressable) emitter sources. This work presents 2D simulation results from VORPAL.[10] The simulation setup and magnetron parameters are provided, and results for both continuous and modulated current sources are presented and discussed.

The conformal finite-difference time-domain (CFDTD) PIC simulation[10] as implemented in VORPAL[11] was used to simulate a ten cavity, rising sun magnetron[12] with cylindrical, five-sided, and ten-sided cathodes. The dimensions of the magnetron and the cathode structures are given in Table I. The simulation was set up with a grid of 102×102 for the cylindrical cathode and 202×202 for the five-sided and ten-sided cathode cases. The higher spatial resolution was needed for proper simulation of the modulated, addressable emitter sources. The macro-particle size was set to 10^6

[a)]Author to whom correspondence should be addressed. Electronic mail: JimBrowning@BoiseState.edu

TABLE I. Rising sun magnetron dimensions used in the simulation for cylindrical and faceted cathodes.

		Facet Width (cm)				
Cathode radius (cm)	Anode radius (cm)	Five-sided	Ten-sided	Small cavity outer radius (cm)	Large cavity outer radius (cm)	Cavity angle (deg)
1.0	2.24	1.18	0.618	6.0	10.0	10.0

electrons per macro-particle. The time step size was typically 2.3 ps, but for the modulated cathode cases, the time step size was set to 1.0 ps to be an integer fraction of the RF period to prevent timing errors. An absorber is used in one of the large cavities to create a load for the RF power. The absorber sets the quality factor, Q, of the magnetron which is 404 for the standard case. Based on the prior results of ICEPIC simulations and studies with VORPAL, the operating parameters for the magnetron were chosen to be a cathode voltage of −22.2 kV and a magnetic field of 0.09 T. Because the primary mode of the rising sun magnetron is the π-mode, no strapping is needed. For the 2D simulations, a linear cathode current density was used. For the results shown here, the current density was set to 326 A/m for the standard case. The current injection model for VORPAL is described here.[13] The simulations showed an oscillating frequency of 960 MHz for the cylindrical cathode and 957 MHz for both the five-sided and ten-sided cathodes; the oscillation of the π-mode was confirmed by looking at the RF axial magnetic field component and by the formation of 5 electron spokes for the ten cavity structure.

For the modulated, addressable current source simulations, each facet plate was divided up into current elements. Each element per facet is turned ON one at a time in sequence at a frequency of 957 MHz. Note that actual gated emitters are not simulated. For the ten-sided cathode, there are two facet plates for every electron spoke. Therefore, the emitter elements were divided into three elements per plate or six elements for two plates (or one spoke). Each element is turned ON for 1/6th of the RF period (1.04 ns) with five elements ON simultaneously. Using this modulation technique, the electrons can be injected at the location and time of the desired electron spokes.

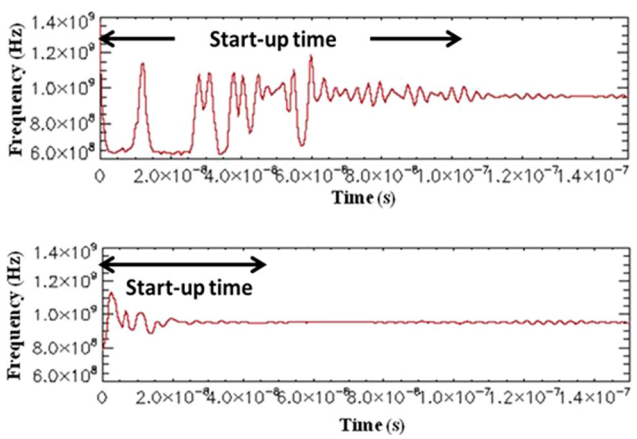

FIG. 1. Frequency vs. time for VORPAL simulation of the ten-sided cathode for (top) the continuous current source and (bottom) the modulated, addressable current source. The start-up time is indicated and is also based on electron spoke formation.

Simulations were first performed for a continuous current source with the three cathode geometries. The results were studied to optimize performance and to compare with the prior ICEPIC results.[7] An important diagnostic tool in VORPAL is the frequency of oscillation of the loaded cavity voltage versus time. An example of this diagnostic is shown in Fig. 1 for a ten-sided cathode with both (a) a continuous current source and (b) a modulated current source with an injected linear current density of 326 A/m. Note the indication of "start-up" time on the figure where the frequency of oscillation appears to be stable and constant. This diagnostic along with visual inspection of the electron spokes was used to determine the start-up time of the magnetron. For the continuous current case shown, the startup time was determined to be ∼110 ns. Shown in Fig. 2 is a plot of the start-up time versus the injected linear current density for the three cathode geometries and for the modulated, ten-sided cathode case. For the continuous current sources, it is observed that the start-up time is relatively constant at 100 ns for current densities above 500 A/m. Space charge effects limit the start-up times for high current densities. Below 500 A/m, the start-up time increases as expected, but the variation in start-up time among the three geometries increases. This variation is believed related to the cathode shape, and it may be possible to optimize the start-up times for each geometry by adjusting the applied static fields. For the cylindrical cathode, start-up below 250 A/m was not observed, and a lower frequency (650 MHz) mode of the device would try to oscillate.

For the modulated, addressable cathode several simulations were performed to study the device behavior and the phase control. First, the oscillations were observed, and as shown in Fig. 1(b), the frequency of the cavity voltage oscillation indicates start-up in less than 60 ns. As seen in Fig. 2, the modulated cathode starts up much faster than the continuous current cathodes with times as short as 35 ns compared to 100 ns for the continuous source. The injected current at

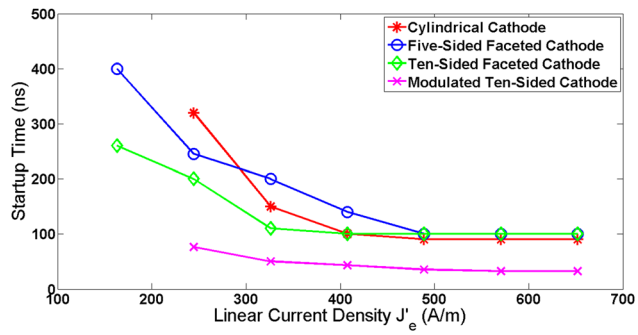

FIG. 2. VORPAL simulation results showing the oscillation startup time vs. injected linear current density for the cylindrical, five-sided, ten-sided, and modulated ten-sided cathodes.

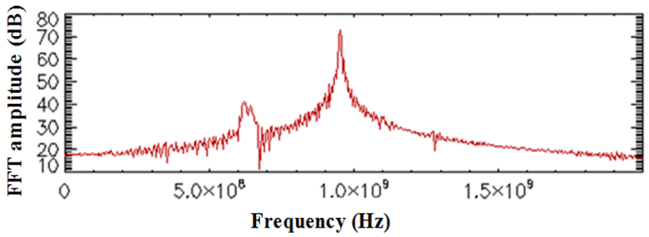

FIG. 3. FFT of the loaded cavity voltage from VORPAL simulation for the modulated, addressable, current source, ten-sided faceted cathode. This plot indicates that the π-mode is dominant at the frequency of operation of 957 MHz. The 650 MHz peak is a cavity mode from the magnetron geometry.

the proper location and time generates bumps, or perturbations, that act to induce oscillation rapidly in the device. This formation is very clear in the simulation images of the electron macro-particles during start-up (not shown). Figure 3 shows the Fast Fourier Transform (FFT) of the cavity voltage over the simulation time of 150 ns, and the 957 MHz peak (π-mode) and the smaller 650 MHz peak are observed.

Next, the locations of the spokes were compared for different simulation runs. If as claimed, the electron injection controls the start-up and spoke locations, then every simulation with the modulated cathode should have the same spoke locations, and hence, RF phase. Shown in Fig. 4 are the electron spokes for two cases: (a) ten-sided with continuous source and (b) ten-sided with modulated source. Three simulations were performed for each case. As seen in Fig. 4(a), the spokes are at random locations for the same simulation time, but for the modulated case in Fig. 4(b) the spokes are at the same locations. Although two of the simulations appear identical, careful inspection will show slight differences. Therefore, these results show that the electron spoke location and resulting RF phase are controlled by the electron injection. This result was also confirmed by comparing the phase of the RF axial magnetic field components in the loaded cavity.

Finally, the electron injection times were changed during a single simulation run. The oscillations are stable after 50 ns. At 88.4 ns, the electron injection times were changed abruptly to generate a 180° phase shift. Shown in Fig. 5 are the electron spokes before the phase shift and then after the phase shift at integer multiples of the RF period. If no phase shift is occurring, the spokes should remain at the same locations, but it is observed that the spokes change location over time until the spokes now align at adjacent cavities compared to the pre-shift case. The spokes have shifted to match the electron injection by 180°. To further analyze this result,

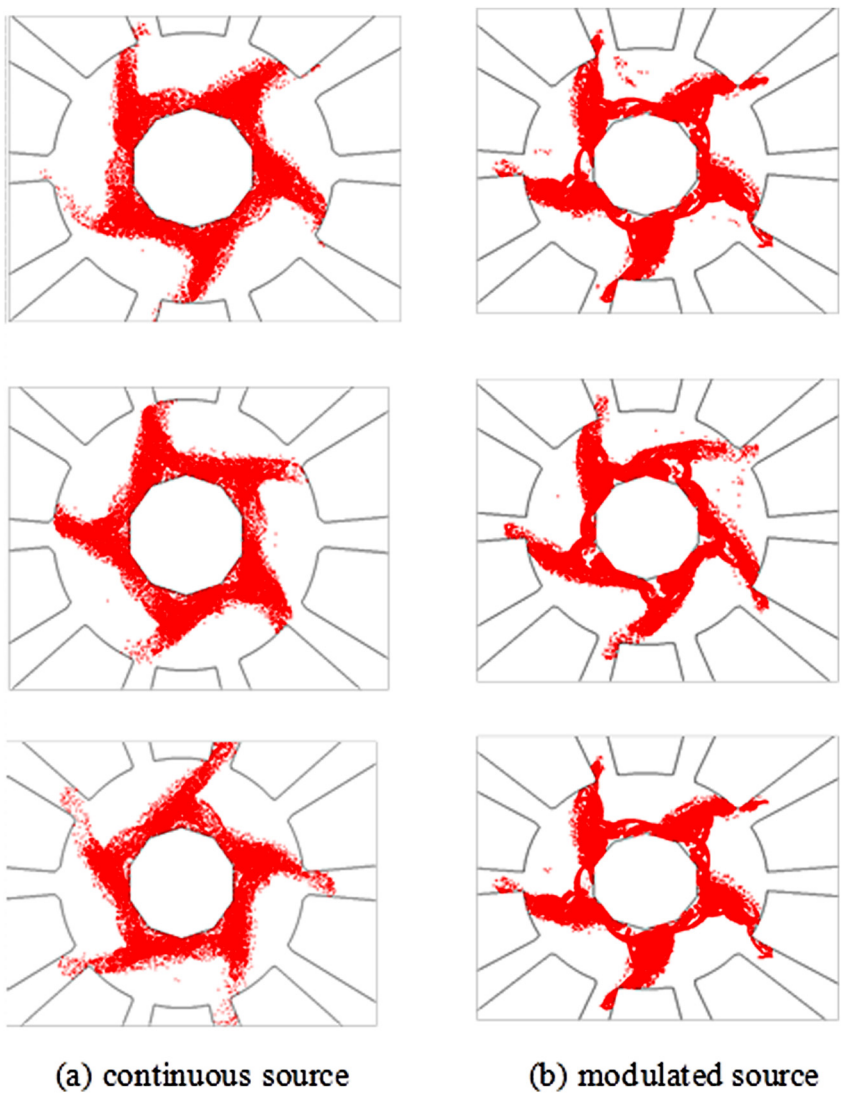

FIG. 4. VORPAL simulation results for the ten-sided cathode for (a) three different runs with a continuous current source at the same capture time (t = 322.12 ns) and for (b) three different runs with a modulated, addressable current source to control phase at the same capture time (t = 76.38 ns). The spokes for the modulated cases are at the same locations while the continuous cases have random spoke locations.

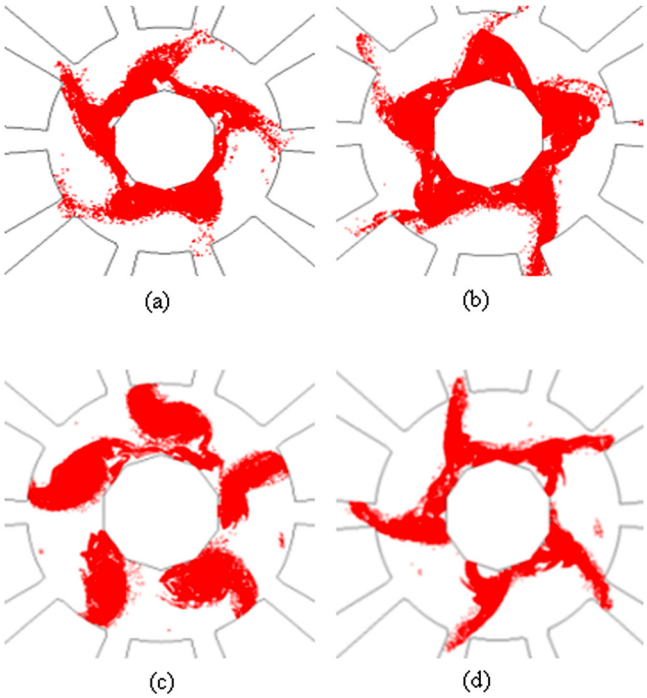

FIG. 5. Ten-sided faceted cathode with modulated addressable current sources, showing transition to a phase shift of 180°. (a) Reference case: Phase = 0° at 82.0 ns, phase shift initiated at 88.40 ns (b) After 14.5 RF periods (t = 96.8 ns) from the reference, 8 RF periods from the phase shift (c) After 17 RF periods (t = 100.0 ns), 11 RF periods from the phase shift. (d) After 35 RF periods (t = 118.4 ns), 29 RF periods from the phase shift.

the RF axial magnetic field components in the loaded cavity were compared with a pre-shift reference time at integer multiples of the RF period, and the phase difference with the pre-shift field was calculated. Figure 6 shows this phase difference versus RF time periods after the phase shift is initiated. The phase shifts 180° in 25 RF cycles for the reference case (Q = 404). The phase shift simulations were also performed for Q = 540 with the phase shift occurring in about 40 RF cycles and for Q = 202 with the phase shift occurring in about 14 RF cycles. It is also important to note that for the lower Q case, the oscillations were less stable, and the spokes were not well formed. The poor spoke quality affected the shape of the phase transition curve as observed in Fig. 6.

Simulations of a ten cavity, rising sun magnetron in 2D have been performed using the CFDTD PIC simulations. The simulations use cylindrical, five-sided, and ten-sided cathodes to represent a device concept using gated field emitters as the electron source. These simulations show that the device oscillates in the π-mode at 960 MHz for the cylindrical cathode and 957 MHz for the faceted cathodes. The start-up times for oscillation were calculated for the three geometries with a minimum start-up time of 100 ns for the best cases. Then, the ten-sided cathode was modulated at the operating frequency using emitter elements spaced along

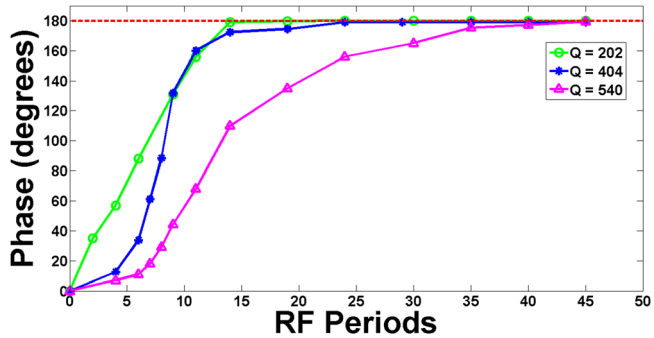

FIG. 6. VORPAL simulation results showing the change in RF phase vs. RF period for different values of Q after a 180° phase shift is generated using the modulated cathode. Phase was determined from the RF B_z component.

the facet plates. Each element was chosen to inject electrons at a time and location to generate the five electron spokes during oscillation. These simulations demonstrated a reduced start-up time with a minimum of 35 ns for the best case. The simulations demonstrated that the electron spokes for the modulated case are at the same location for every simulation run indicating phase control. Driving a 180° phase shift with the electron injection was demonstrated within a run showing that active phase control is possible with a magnetron. Future work will look at overlapping the electron pulses in time, combining continuous current with modulated current, and modifying the simulations for 3D.

This work was supported by the Department of Electrical and Computer Engineering at Boise State University. The authors would like to thank John Luginsland from the Air Force Office of Scientific Research for encouraging this work.

[1]R. J. Barker, J. H. Booske, N. C. Luhmann, and G. S. Nusinovich, *Modern Microwave and Millimeter-Wave Power Electronics* (John Wiley & Sons, Inc., Piscataway, NJ, 2005).
[2]G. B. Collins, *Microwave Magnetrons* (McGraw-Hill, New York, 1948).
[3]D. A. Shiffler, J. W. Luginsland, M. Ruebush, M. LaCour, K. Golby, K. Cartwright, M. Haworth, and T. Spencer, IEEE Trans. Plasma Sci. **32**(3), 1262–1266 (2004).
[4]M. C. Jones, V. B. Neculaes, Y. Y. Lau, R. M. Gilgenbach, and W. M. White, Appl. Phys. Lett. **85**(26), 6332–6334 (2004).
[5]M. Fuks and E. Schamiloglu, Phys. Rev. Lett. **95**(20), 205101 (2005).
[6]M. C. Jones, V. B. Neculaes, Y. Y. Lau, R. M. Gilgenbach, W. M. White, B. W. Hoff, and N. M. Jordan, Appl. Phys. Lett. **87**(8), 081501 (2005).
[7]J. Browning and J. Watrous, J. Vac. Sci. Technol., B **29**(2), 02B109 (2011).
[8]D. Whaley, R. Duggal, and C. Armstrong, IEEE Trans. Electron Devices **56**(5), 896–905 (2009).
[9]R. Peterkin and J. W. Luginsland, Comput. Sci. Eng. **4**(2), 42–49 (2002).
[10]M. C. Lin, C. Nieter, P. H. Stoltz, and D. Smithe, Open Plasma Phys. J. **3**, 48–52 (2010).
[11]C. Nieter and J. R. Cary, J. Comput. Phys. **196**(2), 448–473 (2004).
[12]R. Moats, Research Laboratory Electronics, Technical Report No. 99, 1949.
[13]M. C. Lin, P. H. Stoltz, D. Smithe, H. Song, H. Jong, J. J. Choi, S. J. Kim, and S. H. Jang, J. Korean Phys. Soc. **60**(5), 731–738 (2012).